Silver(I)-Selective Thioether Ligands. Solution NMR and X-ray Structural Studies on the Interaction of 2,5,8-Trithia[9]-*m*-cyclophane and Related Ligands with Silver(I)

Jaume Casabó,[1a] Teresa Flor,[1a] M. N. Stuart Hill,[1b] Hilary A. Jenkins,[1c] Joyce C. Lockhart,*[,1b] Stephen J. Loeb,*[,1c] Isobel Romero,[1a] and Francesc Teixidor*[,1a]

Department of Chemistry, Bedson Building, University of Newcastle upon Tyne, Newcastle upon Tyne NE1 7RU, U.K., Department of Chemistry and Biochemistry, University of Windsor, Windsor, Ontario, Canada N9B 3P4, and ICMAB, Campus Universitat Autonoma, Bellaterra 08193, Spain

Received March 24, 1995[⊗]

The reaction of 2,5,8-trithia[9]-*m*-cyclophane (L^1) with $AgCF_3SO_3$ in a 1:1 ratio produced the polymeric material $\{[Ag(L^1)][CF_3SO_3]\cdot CH_3CN\}_x$. This polymer crystallized in the space group $P2_1/c$ with $a = 11.218(2)$ Å, $b = 11.317(3)$ Å, $c = 17.035(7)$ Å, $\beta = 104.17(2)°$, $V = 2097(2)$ Å^3, and $Z = 4$. The structure refined to $R = 4.11\%$ and $R_w = 5.69\%$ for 1261 reflections with $F_o^2 > 3\sigma(F_o^2)$. NMR solution data indicate a multiplicity of solution structures in rapid exchange. The exchange of L^1 and analogues with their respective silver complexes in CD_3CN/CD_2Cl_2 was examined by NMR spectroscopy. The L^1 exchange on silver was shown by the dilution method to be D or I_D in character.

Introduction

The ligands 2,5,8-trithia[9]-*m*-cyclophane (L^1) and 5-oxa-2,8-dithia[9]-*m*-cyclophane (L^2) have been found to be useful in establishing good selectivity for silver ions in ion selective electrodes[2,3] and have many interesting complexes, particularly with late transition soft metals.[4−6] At one stage, we sought

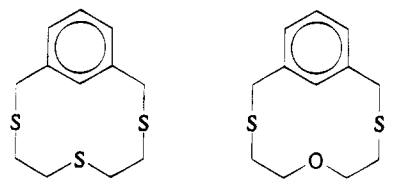

evidence that the silver formed a macrocyclic complex with L^1 or L^2. However, later work showed the most impressive selectivity[7] with the simple thioethers 1,3-bis(2-thiabutyl)-benzene (L^3) and ethyl phenyl thioether (L^4), which seems to be related to the existence of a thioether moiety in the sensing molecule and must be associated with kinetic events. In the selective processes which arise in membranes (ISE and the three-phase transport), there is an organic phase which contains the selective ligand in contact with an aqueous solution of metal ion. At the interface, the process

$$mAg^+(aq) + mL \rightarrow (AgL^+)_m \quad (1)$$

must occur. The question is how the *selectivity* of L for Ag over other metals is achieved. Earlier work concentrated on the kinetics of ligand exchange processes such as eqs 2 (associative process) and 3 (dissociative process) occurring in

$$L + [AgL^+] \underset{k_{-2}}{\overset{k_2}{\rightleftharpoons}} [LAg^+] + L \quad (2)$$

$$Ag^+ + L \underset{k_{-3}}{\overset{k_3}{\rightleftharpoons}} [AgL^+] \quad (3)$$

similar ligand−metal systems.[8,9] In ISE or other three-phase processes, ligand exchange can only happen in excess ligand, i.e. in the membrane itself. This paper describes some NMR investigations of model systems which examine this AgL exchange for ligands L^1 and L^2, for which a suitable NMR-exchangeable label was found.[10] A knowledge of the kinetics of the reaction for silver and for relevant competitor ions will be helpful in pinpointing the origins of selectivity.

Abel, Orrell, and Bhargava[11] have reviewed the many processes postulated and observed (usually by NMR techniques) for sulfur ligands in coordination with metal ions. These include inversions at sulfur as well as ring-flexing. On coordination to a metal ion, the activation energy for the sulfur inversion is expected to fall.[11] Additional processes to be expected in the metal-containing systems include intramolecular ring shifts of

⊗ Abstract published in *Advance ACS Abstracts,* October 1, 1995.

(1) (a) ICMAB. (b) University of Newcastle. (c) University of Windsor.
(2) Casabó, J.; Mestres, L.; Eschriche, L.; Teixidor, F.; Perez-Jiménez, C. *J. Chem. Soc., Dalton Trans.* **1991**, 1969.
(3) Lockhart, J. C.; Mousley, D. P.; Hill, M. N. S.; Tomkinson, N. P.; Teixidor, F.; Almajano, M. P.; Escriche, L.; Casabó, J. F.; Sillanpää, R.; Kivekäs,R. *J. Chem.Soc., Dalton Trans.* **1992**, 2889.
(4) de Groot, B.; & Loeb, S. J; *Inorg. Chem.* **1990**, *29*, 4084.
(5) de Groot, B.; Hanan, G. S.; Loeb, S. J. *Inorg. Chem.* **1991**, *30*, 4644.
(6) Kickham, J. E.; Loeb, S. J. *Inorg. Chem.* **1994**, *33*, 4351.
(7) Teixidor, F.; Flores, M. A.; Eschriche, L.; Viñas, G.; & Casabó, J. *J. Chem. Soc., Chem. Commun.* **1994**, 963.
(8) Lockhart, J. C.; McDonnell, M. B.; Hill, M. N. S.; Todd, M. *J. Chem. Soc., Perkin Trans. 2,* **1989**, 1915.
(9) Lockhart, J. C.; Clegg, W.; Hill, M. N. S.; Rushton, D. J. *J. Chem. Soc., Dalton Trans.* **1990**, 3541.
(10) Romero, I.; Unpublished work.
(11) Abel, E. W.; Orrell, K. G.; Bhargava, S. K. *Prog. Inorg. Chem.* **1984**, *32*, 1.

0020-1669/95/1334-5410$09.00/0

the position of the metal coordination to the ligand and intermolecular switching of metal between ligands. This latter process may include a full dissociation step (first order) as shown in eq 3 or be bimolecular as suggested in eq 2. To our knowledge, no detailed analysis of the dynamics of silver–thiamacrocycle complexes has yet been made. This paper attempts to identify the processes revealed by NMR studies at low temperatures in the mixtures of silver salts with L^1–L^3 and to relate these to structural information, from solution NMR studies. A crystal structure determination of one of the complexes of L^1 obtained from acetonitrile solution is described.

Experimental Section

Materials. The ligands L^1–L^3 were prepared as described previously.[2-6]

Instruments. NMR Spectra were run on Bruker WM300-WB, AC400, and WP200 spectrometers. All ^{13}C spectra were broad-band decoupled. The variable-temperature (VT) and HETCOR spectra were obtained on the WM300-WB. The solvent used for VT work was an equal-volume mixture of CD_3CN and CD_2Cl_2. Kinetic analysis was performed with an in-house program for simulating exchange of two uncoupled sites or with DNMR3.[12] The FAB mass spectrum was obtained from a *m*-nitrobenzyl alcohol solution of the silver complex of L^1 on a KRATOS M58ORF instrument. Operating conditions were accelerating voltage 4 kV and atom beam 8 kV with xenon bombarding atoms.

Preparation of Silver Chelates of L^1 and L^2. The silver trifluoromethanesulfonate (triflate) complex of L^1 precipitated from an NMR sample containing equimolar quantities of ligand and silver salt in equal volumes of CD_3CN and CD_2Cl_2, as a white powder, blackening on exposure to sunlight. The powder was dried in vacuo overnight; mp 228 °C. Anal. Calcd for $C_{13}H_{16}AgF_3O_3S_4$: C, 30.4; H, 3.1. Found: C, 30.6; H, 3.0. Mass spectra showed a parent ion for LAg at *m/z* 363, 365 and $[LAg]_2 + CF_3SO_3 + H$ at low intensity (*m/z* 876, 878, 880).

Preparation of $\{[Ag(L^1)][CF_3SO_3]\cdot CH_3CN\}_x$. L^1 (100 mg, 0.390 mmol) and $AgCF_3SO_3$ (100 mg, 0.390 mmol) were mixed together in CH_3CN (25 mL), and the resulting clear solution was stirred in the dark for 1 h. The volume of the solution was reduced to *ca.* 10 mL. Vapor diffusion of diethyl ether into this solution produced colorless crystals of the product suitable for X-ray analysis. Yield: 180 mg (90%). ^1H NMR (δ, CD_3CN,300K): 8.02 (s, 1H, aromatic), 7.37 (m, 3H, aromatic), 3.99 (s, 4H, benzylic), 2.72 (t, 4H, SCH_2), 2.29 (t, 4H, SCH_2). $^{13}C\{^1H\}$ NMR (δ, CD_3CN, 300 K): 139.61, 128.50, 128.00 (aromatic), 36.17 (benzylic), 31.03, 29.20 (SCH_2). Anal. Calcd for $C_{15}H_{19}AgF_3NO_3S_4$: C, 32.49; H, 3.46. Found: C, 32.40; H, 3.42.

Synthesis of $[Ag(L^2)]CF_3SO_3$. To a solution of L^2 (0.1 g, 0.41 mmol) in dry methanol (50 mL) was added $AgCF_3SO_3$ (0.105 g, 0.41 mmol), and the solution was taken to reflux for 2 h. The resulting solution was filtered, and the filtrate was slowly concentrated (4 days) to obtain a white precipitate, which was filtered off and dried. Yield: 0.125 g (61%). ^1H-NMR (δ, 400 MHz, $CDCl_3$, 25 °C) : 8.15 (s, 1), 7.21 (m, 3), 3.88 (s, 4), 2.88 (app (apparent) t, 4), 2.70 (app t, 4). Anal. Calcd for $C_{13}H_{16}AgF_3O_4S_3$: C, 31.37; H, 3.22; S, 19.34. Found: C, 32.52; H, 3.56; S, 19.40.

Synthesis of $[Ag(L^2)_2]CF_3SO_3$. The procedure was as before but a L^2/Ag ratio of 2/1 was used, starting from 0.2 g of L^2. Yield: 0.210 g (69%). ^1H NMR (δ, 400 MHz, $CDCl_3$, 25 °C): 8.06 (s, 1), 7.22 (m, 3), 3.86 (2, 4), 2.90 (app t, 4), 2.67 (app t, 4). Anal. Calcd for $C_{25}H_{32}AgF_3O_5S_5$: C, 40.66; H, 4.33; S, 21.73. Found: C, 40.57; H, 4.55; S, 21.61.

General X-ray Crystallography. Diffraction experiments were performed on a four-circle Rigaku AFC6S diffractometer with graphite-monochromatized Mo Kα radiation. The unit cell constants and orientation matrix for data collection were obtained from 25 centered reflections ($15° < 2\theta < 35°$). Machine parameters, crystal data, and data collection parameters are summarized in Table 1. The intensities of three standard reflections were recorded every 150 reflections and showed no statistically significant changes over the duration of the data collections. The intensity data were collected using the ω–2θ scan technique, in four shells ($2\theta < 30$, 40, 45, 50°). The empirical absorption coefficient was relatively small, and an absorption correction (ψ scans) was applied to the data. The data were processed using the TEXSAN software package running on an SGI Challenge XL computer.[13] Refinement was carried out by using full-matrix least-squares techniques on F by minimizing the function $w(|F_o| - |F_c|)^2$, where $w = 1/\sigma^2(F_o)$ and F_o and F_c are the observed and calculated structure factors. Atomic scattering factors[14] and anomalous dispersion terms[15,16] were taken from the usual sources. Fixed H atom contributions were included with C–H distances of 0.95 Å and thermal parameters 1.2 times the isotropic thermal parameters of the bonded C atoms. No H atoms were refined, but all values were updated as refinement continued.

Structure of $\{[Ag(L^1)][CF_3SO_3]\cdot CH_3CN\}_x$. Colorless crystals of the complex were grown by vapor diffusion of diethyl ether into a solution of the complex as described in the preparative procedure. Statistical analysis of intensity distributions and a determination of observed extinctions were consistent with the space group $P2_1/c$. This

Table 1. Summary of Crystal Data, Intensity Collection, and Structure Refinement for $\{[Ag(L^1)][CF_3SO_3]\cdot MeCN\}_x$

formula	$C_{15}H_{19}AgF_3NO_3S_4$	Z	4
fw	554.42	μ, cm^{-1}	13.8
a, Å	11.218(2)	λ, Å	0.7017
b, Å	11.317(3)	*T*, °C	23
c, Å	17.035(7)	goodness of fit	1.68
β, deg	104.17(2)	R,[a] %	4.11
space group	$P2_1/c$ (No. 14)	R_w,[b] %	5.69
V, $Å^3$	2097(2)		
ρ, g/cm^3	1.76		

[a] $R=\sum||F_o| - |F_c|/\sum|F_o||$. [b] $R_w = (\sum w(|F_o| - |F_c|)^2/\sum wF_o^2)^{1/2}$ and $w = 1/\sigma^2(F)$.

Table 2. Selected Positional and Thermal Parameters for $\{[Ag(L^1)][CF_3SO_3]\cdot CH_3CN\}_x$

atom	*x*	*y*	*z*	*B*(eq), $Å^2$
Ag1	0.1017(1)	0.0135(1)	0.18348(7)	4.52(7)
S1	0.1412(4)	−0.1998(4)	0.1499(3)	4.1(2)
S2	−0.0760(4)	−0.2084(4)	−0.1084(3)	3.8(2)
S3	0.1299(4)	−0.5221(4)	−0.1631(2)	3.8(2)
C7	0.290(1)	−0.205(1)	0.1246(9)	3.9(8)
C8	0.038(1)	−0.250(1)	0.0593(9)	3.9(8)
C9	0.024(2)	−0.164(1)	−0.013(1)	3.9(9)
C10	0.020(1)	−0.298(1)	−0.1554(8)	3.0(7)
C11	0.028(1)	−0.426(1)	−0.1265(9)	4.0(8)
C12	0.280(1)	−0.458(1)	−0.1185(9)	4.1(8)

Table 3. Selected Bonding Parameters for $\{[Ag(L^1)][CF_3SO_3]\cdot CH_3CN\}_x$

	Distances (Å)		
Ag–S1	2.545(5)	Ag–S2	2.530(5)
Ag–S3	2.556(4)	S1–C7	1.82(1)
S1–C8	1.78(2)	S2–C9	1.81(2)
S2–C10	1.80(1)	S3–C11	1.80(1)
S3–C12	1.82(2)	C2–C12	1.51(2)
C6–C7	1.49(2)	C8–C9	1.55(2)
C10–C11	1.53(2)		
	Angles (deg)		
S1–Ag–S2	135.9(1)	S1–Ag–S3	106.3(2)
S2–Ag–S3	117.0(2)	C7–S1–C8	102.9(7)
C9–S2–C10	104.5(7)	C11–S3–C12	102.5(7)
S1–C7–C6	110(1)	S1–C8–C9	114(1)
S2–C9–C8	117(1)	S2–C10–C11	113(1)
S3–C11–C10	117(1)	S3–C12–C2	112(1)

(12) DNMR3: Kleier, D. A., Binsch, G. *J. Magn. Reson.* **1970**, *3*, 146.
(13) TEXSAN-TEXRAY Structure Analysis Package, Molecular Structure Corp., (1985).
(14) Cromer, D. T.; Waber, J. T. *International Table for X-ray Crystallography*; Kynoch Press: Birmingham, England, **1974**; Vol. IV, Table 2.2A.
(15) Ibers, J. A.; Hamilton, H. A. *Acta Crystallogr.* **1974**, *17*, 781.
(16) Cromer, D. T. *International Table for X-ray Crystallography*; Kynoch Press: Birmingham, England, **1974**, Vol. IV, Table 2.3.1.

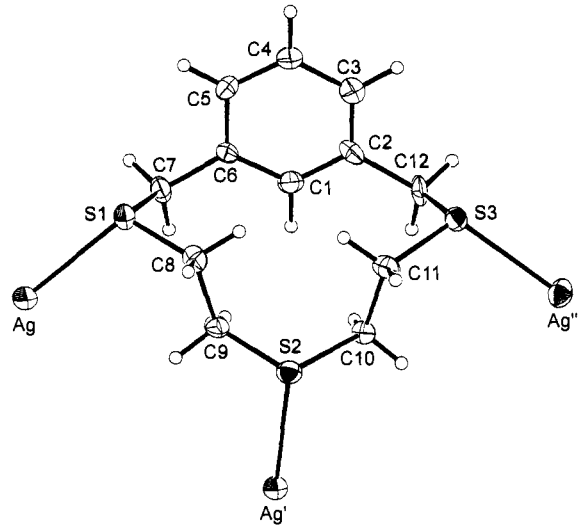

Figure 1. Perspective ORTEP drawing of the repeating $[Ag(L^1)]^+$ unit showing the three symmetry-related silver atoms and the atom-numbering scheme. Thermal ellipsoids of 30% probability are shown.

assignment was confirmed by successful solution and refinement of the structure. A total of 3906 reflections were collected, and 1261 unique reflections with $F_o^2 > 3\sigma(F_o^2)$ were used in the refinement. The positions of the silver and sulfur atoms were determined by direct methods from the initial E maps with highest figure of merit. The remaining non-hydrogen atoms were located from difference Fourier map calculations. In the final cycles of refinement, the silver, sulfur, and carbon atoms were all assigned anisotropic thermal parameters. This resulted in $R = 0.0411$ and $R_w = 0.0569$ at final convergence. The Δ/σ value for any parameter in the final cycle was less than 0.001, and a final difference Fourier map showed maximum and minimum residuals of +0.76 (Ag atom) and −0.69 e/Å^3. Selected atomic positional parameters are summarized in Table 2, and selected bond distances and angles are summarized in Table 3. Full listings of atomic positional parameters (Table S-2), nonessential bonding parameters (Table S-3), thermal parameters (Table S-4), and hydrogen atom parameters (Table S-5) are deposited as Supporting Information.

Results

Synthesis. The interaction of silver salts with ligands L^1 and L^2 produced one-ligand chelates AgL^1, and AgL^2, two-ligand chelates AgL^2_2, and an acetonitrile AgL^1 solvate, depending on conditions. The first three compounds were dried in vacuo and characterised analytically. The fourth was also characterized crystallographically.

X-ray Structure of $\{[Ag(L^1)][CF_3SO_3]\cdot CH_3CN\}_x$. The X-ray structure of this acetonitrile solvate shows that, in the solid state, the reaction of silver triflate with L^1 produces a polymeric material in which all three of the sulfur atoms are exodentate and coordinated to a Ag^+ ion: Ag−S(1) 2.545(5), Ag′−S(2) 2.530(5), Ag″−S(3) 2.556(5) Å; S(1)−Ag−S(2) 135.9(1), S(1)−Ag−S(3) 106.3(2), S(2)−Ag−S(3) 117.0(2)°. The polymer forms cationic sheets with anions and MeCN solvent molecules between the sheets and loosely associated with the Ag^+ ion: Ag···N(1) 2.85(2), Ag···O(1) 2.66 Å. A perspective ORTEP drawing of the repeating unit is shown in Figure 1; the coordinated silver atoms Ag, Ag′ and Ag″ are related by symmetry. The conformation of L^1 is very similar to that observed in the crystal structure of the free ligand, with only small deviations observed in the torsional angles (Table 4). The coordination sphere of the silver is shown in Figure 2, indicating interaction with L^1, triflate, and with acetonitrile. In Figure 3 a packing diagram shows the unit cell, and the sheetlike polymeric structure with anions and solvent molecules between the layers.

Table 4. Torsional Angles[a] Associated with L^1 in $\{[Ag(L^1)][CF_3SO_3]\cdot CH_3CN\}_x$

bonds	angle, deg	bonds	angle, deg
S1−C7−C6−C1	108(2)	C9−S2−C10−C11	84(1)
S1−C7−C6−C5	−69(2)	S2−C10−C11−S3	−175.5(7)
C6−C7−S1−C8	−50(1)	C10−C11−S3−C12	65(1)
C7−S1−C8−C9	−68(1)	C2−C12−S3−C11	54(1)
S1−C8−C9−S2	178.6(8)	S3−C12−C2−C1	−108(2)
C8−C9−S2−C10	−85(1)	S3−C12−C2−C3	67(2)

[a] The sign is positive if, as viewed from atom 2 to atom 3, a clockwise motion of atom 1 would superimpose it on atom 4.

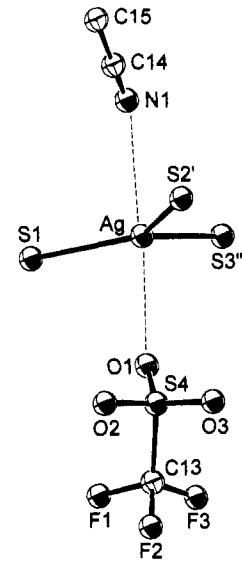

Figure 2. Perspective ORTEP drawing of the Ag^+ coordination sphere showing interaction of the thiacyclophane ligands, triflate anion, and acetonitrile solvent molecule with the metal center. Thermal ellipsoids of 30% probability are shown.

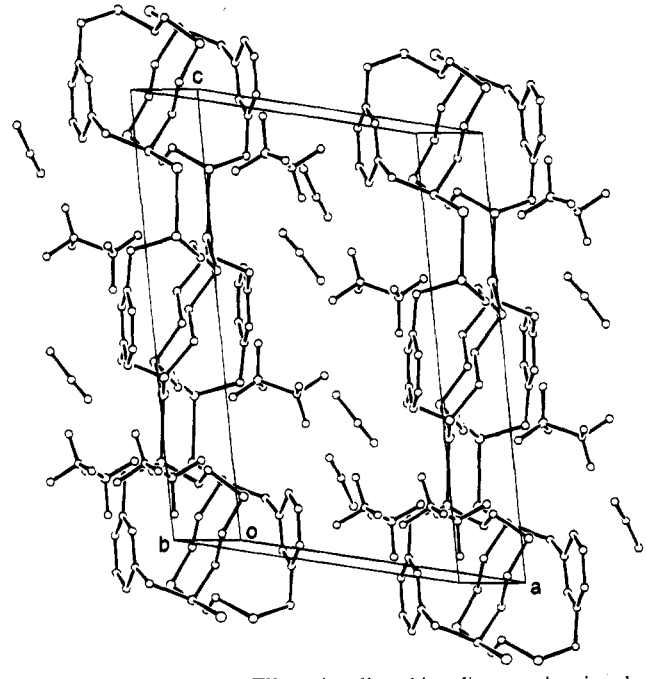

Figure 3. Perspective ORTEP unit cell packing diagram showing the sheetlike polymeric nature of the cations and the positioning of the solvent and anions between these cationic layers.

NMR Results. Each of the ligands L^1−L^3 was studied extensively by ^1H and ^{13}C NMR spectroscopy in the presence and absence of silver triflate and other salts of silver. Table 5 shows the numbering of the carbons used in identification. The

Table 5. HETCOR Assignments of ^{13}C and ^{1}H Shifts for L^1 and L^2 (ppm)[a]

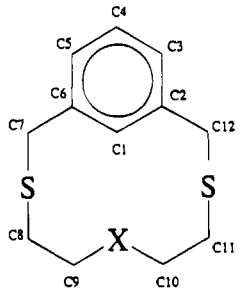

	L^1 [b]	L^2 [b]		L^1 [b]	L^2 [b]
C2[c]	135.9	138.6	C9 (H9)	29.05 (2.3)	67.11 (3.0)
C1 (H1)	130.5 (7.27)	130.1 (7.75)	C8 (H8)	30.69 (2.4)	28.78 (2.50)
C3 (H3)	127.4 (7.45)	127.5 (7.28)	C7 (H7)	35.67 (3.9)	39.76 (3.8)
C4 (H4)	129.8 (7.55)	128.97 (7.35)			

[a] Obtained on the Bruker WM300-WB in 1/1 CD_3CN/CD_2Cl_2. [b] ^{1}H shifts in parentheses. [c] Only one shift for each equivalent pair of atoms is given.

protons are numbered analogously. It was noticed that, for the signal for H1, the aromatic hydrogen projecting into the macrocyclic cavity, there was a dramatic shift downfield (7.2 to 8.0 ppm for L^1; 7.7 to 8.1 ppm for L^2) when 1 equiv of silver salt was added. The open-chain ligand L^3 showed no corresponding shift. The magnitude of this shift change (together with lesser shifts of protons on C7(C12), C8(C11), C9(C10)) suggested a strong interaction of silver with the sulfur of the alicyclic ring (of L^1 or L^2) such that the unique H1 proton was strongly affected by the proximity of the silver. This suggested at one stage that silver actually coordinated to the ring in an endodentate fashion. However, the crystal data for the solvate reported in this paper show that L^1 can form polymeric complexes in which silver ions bridge different rings. Such structures do not appear to account for the solution observations. The solution behavior was probed further with NMR methods.

A HETCOR analysis for L^1 and L^2 allowed the assignment of the ^{13}C signals shown in Table 5. Signals assigned to carbons C2(C6) and C9(C10) were strongly shifted when silver salts were added. At 210 K, a solution of L^1 had sharp signals at 135.9 (C2), 129.7 (C1), 129.3 (C4), 126.4 (C3), 33.2 (C7), 28.8 (C8), and 28.2 (C9) ppm. The chelate $[AgL^1]^+$ at 210 K had corresponding signals at 139.4 (C2), 129.0 (C1, C4), and 127.4 (C3) in the aromatic region and 35.4 (C7), 29.3 (C8), and 26.7 (C7). The equimolar mixture of the two showed averaged signals at room temperature and pairs of signals at low temperatures which for C2 and C9 were suitable for kinetic analysis. Figure 4 gives details of the assignments of signals used in the kinetic study. The low-temperature spectra of an equimolar mixture of L^1 and $[AgL^1]^+$ are shown, with relevant assignments.

The NMR titration of L^1 or L^2 with silver salts at room temperature, performed with ^{1}H and ^{13}C spectra, indicated a smooth change of shift as the silver salt was added up to the AgL complex formation. Subsequent slight changes were observed as further equivalents of silver were added, suggesting multinuclear complexes could be present in excess silver salt. Typical data are given in Table 6 for L^2 in acetonitrile at ambient temperature with $AgBF_4$.[17]

Compositions between free ligand and AgL complex were investigated by variable-temperature ^{13}C NMR spectroscopy.

(17) A reviewer suggests the data approximately follow what is expected for a stability constant of $\log(K/L\ mol^{-1}) \approx 3$ for the complex AgL^2.

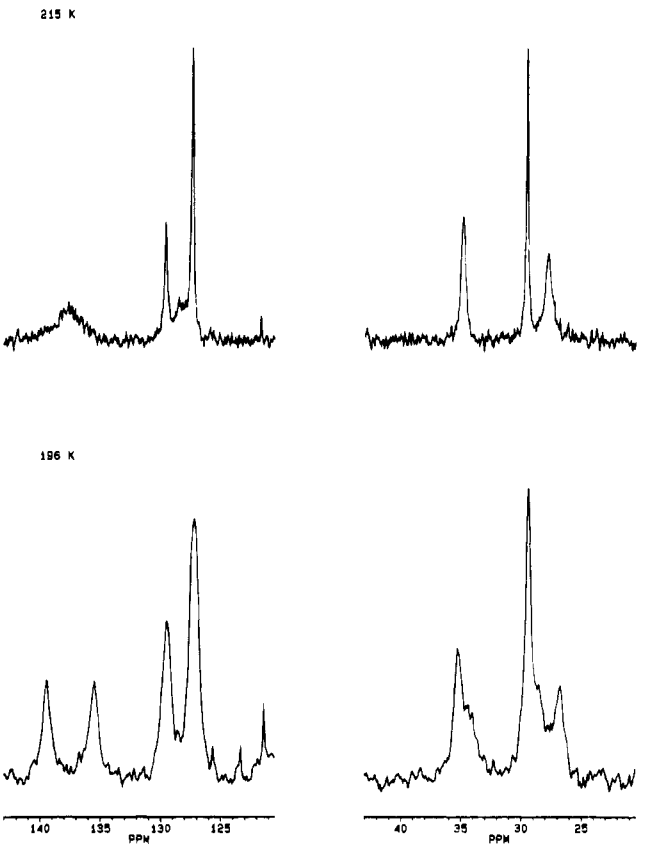

Figure 4. ^{13}C NMR spectra of equimolar L^1 with $[AgL^1]^+$ in CD_3CN/CD_2Cl_2. Lower trace shows a decoalesced pair of signals for C2(AgL^1), C2(L^1) at 139 and 136 ppm and another for C9(L^1), C9(AgL^1) at 29 and 26.9 ppm. Upper trace shows these pairs of signals coalesced at 215 K. Components of the CF_3 quartet (triflate) are also seen.

Table 6. Proton NMR Shifts of the H1 Proton of L^2 on Titration with Silver Tetrafluoroborate[a]

[Ag], M	[Ag]/L^2	shift, ppm	[Ag], M	[Ag]/L^2	shift, ppm
0.000	0/1	7.66	0.015	1.5/1	8.15
0.003	0.33/1	7.8	0.020	2/1	8.19
0.005	0.5/1	7.9	0.030	3/1	8.21
0.007	0.66/1	7.95	0.040	4/1	8.21
0.010	1/1	8.05			

[a] Spectra recorded in CD_3CN at 21 °C taken on the Bruker AC400.

The signals originally appearing at 135.9 (C2) and 28.2 (C9) ppm at 210 K (for L^1) were shifted in the AgL^1 complex to 139.4 and 26.9 ppm. For mixtures at room temperature, an averaged signal for each pair of free and complexed L^1 signals was seen, which decoalesced at temperatures from 210 to 190 K (shown in Figure 4). At low temperatures in the spectra of all mixtures (L^1 or L^2) with silver ions present additional signals from the CF_3 quartet of the triflate ion were observed.

Kinetic Analysis for L^1. The coalescence points of the 1/1 mixture of ligand L^1 and chelate AgL^1 for the signals of C2(C6) and C9(C10) were observed at 211 and 202 K respectively, giving $\Delta G^{\ddagger}_{202-211} = 9.5$ kcal m^{-1}. The mixtures with $[L^1]/[AgL^1]$ of 1 and 0.33 were examined, and the rate constants obtained by simulation are shown in Table 7. The value of T_2 (transverse relaxation time) required as input for the line shape simulations was obtained by cooling solutions of free L^1 to the lowest temperature (196 K) which avoided precipitation. This line width may be viscosity dependent, and may represent a site undergoing sulfur inversions, ring whizzing, etc. The natural line width in the aliphatic region was greater than that

Table 7. Rate Constants for the Exchange of 0.025 M AgL^1 with 0.025 M L^1 [a]

T, K	k, s^{-1}	T, K	k, s^{-1}
215	950[b]	202	250[b,c]
211	680[b,c]	200	170[b]
207	380[b]		

[a] Solvent 1/1 CD_3CN/CD_2Cl_2; Arrhenius energy 9.5 kcal mol^{-1}. [b] From simulation. [c] Obtained from coalescence temperature by the Gutowsky–Holm approximation.

for the aromatics, but no separation of signals was observed. The apparent line width for the $[AgL^1]$ complex was wider than that for the free ligand L^1. The selected tracking signal (C9) at 26.9 and 29 ppm unfortunately overlapped another aliphatic signal at 30 ppm (see Figure 4), so that only one side of the spectrum could be fitted adequately. One aromatic signal for $[AgL^1]$ decoalesced at temperatures around 220–200 K (above the temperature of the ligand exchange we were investigating). The process which caused this was probably a ring shift, since it involved the unique C1. The resolved exchange components for this signal interfered with the L^1 signal at 135.9 ppm needed for kinetic analysis of the 3/1 $[AgL^1]/[L^1]$ mixture. Thus reliable line shape simulations were only obtained for the 1/1 mixture and at 202 K for the 3/1 mixture. For the application of the Shchori method[8,9,18] at least two ratios of [AgL]/[L] were required to permit us to assess the relative contribution of eqs 2 and 3 to the overall metal exchange process. For dissociative (D or I_D) (eq 3, reverse) and bimolecular (A or I_A) (eq 2) steps operating together, eq 4 holds in excess ligand. A plot of k_{obs}/

$$k_{obs} = k_2[AgL] + k_{-3}[AgL]/[L] \quad (4)$$

[AgL] versus 1/[L] will give the second-order rate constant k_2 as the intercept (if any) and the first-order dissociative rate constant k_{-3} (if any) as the slope. These plots are subject to large errors but allow a mechanistic distinction. The data at 202 K in Table 7 indicate a straight line with zero intercept, and so a D or I_D mechanism.

In the examples examined previously,[8,9] the second-order path was dominant at the concentrations required for NMR investigations. However the relative turnover of reaction by second-order and first-order routes must be concentration-dependent. Another experiment which yields information as to whether any process of kinetic order greater than first is present is the dilution method, recently used by Detellier et al.[19] This does not necessarily indicate whether a first-order process is competitive at all, or at what concentration, unless the first-order process is the only one present. Solutions initially containing 0.025 M AgL and 0.025 M L were examined at 211 K, the coalescence point for the C2 signals. Spectra after serial dilution to 0.0125 M and then to 0.0062 M in each component showed almost no change (see Figure 5), showing that there was no determinable second-order path. The exchange of ligand in this system thus occurs by a D or I_D mechanism. The dissociative mechanism is also anticipated to be occurring in the presence of excess silver ions (as would be present at the membrane interface in an ISE).

The oxa ligand L^2 was also investigated. Spectra obtained for the free ligand on cooling in the CD_3CN/CD_2Cl_2 solvent showed signs of a process affecting the signal of the unique hydrogen (H1) and OCH_2 hydrogen, but it was not slowed sufficiently at 190 K for investigation. The complex with silver

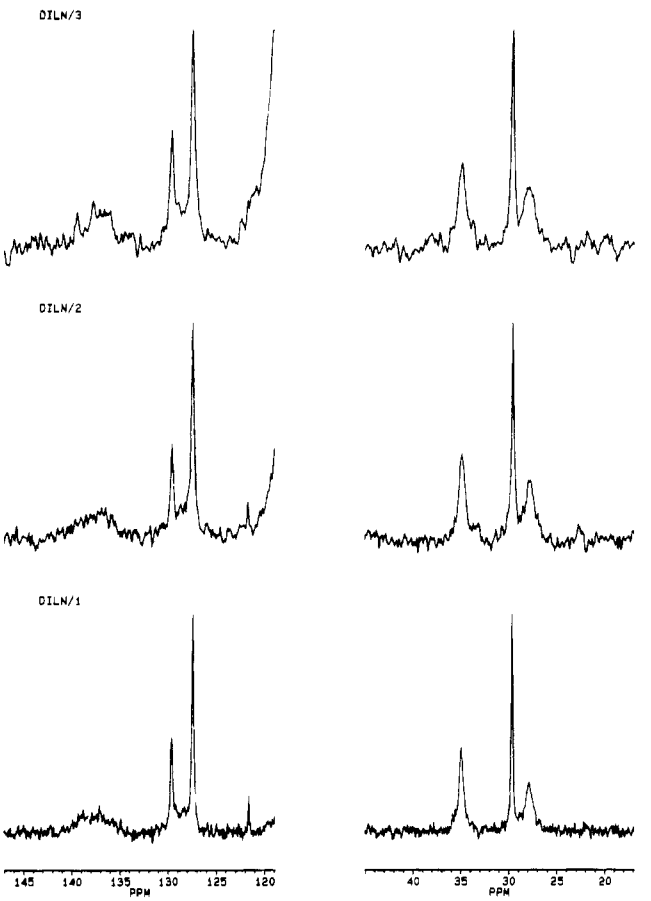

Figure 5. ^{13}C NMR spectra of equimolar mixtures of L^1 with $[AgL^1]^+$ in CD_3CN/CD_2Cl_2 at 211 K at different total ligand concentrations of 0.0138 M (top), 0.0253 M (middle), and 0.05 M (bottom).

Table 8. Rate Constants for the Exchange of 0.009 M AgL^2 with 0.008 M L^2 [a,b]

T, K	k, s^{-1}	T, K	k, s^{-1}
220	9600	200	2180
210	5150	190	950

[a] Solvent 1/1 CD_3CN/CD_2Cl_2. [b] From simulation.

triflate exchanged with free ligand at a rate some 10 times faster than for the corresponding L^1, so that the ^{13}C spectra did not show separate signals for AgL and for L at the lowest temperature reached (190 K). Rate constants could be obtained from the increasing line width of the unique H1 signal as temperature was lowered, by simulation of the signal with DNMR3. The rate constants are shown in Table 8.

The behavior of the third ligand L^3 provided a contrast. None of the ^1H or ^{13}C signals moved sufficiently in the presence of silver triflate to provide a window on kinetic behavior. In particular, the unique hydrogen H1 did not show a large shift as was the case for L^1 and L^2.

Discussion

The structure of the free ligand L^1, determined in the solid state, indicates a bracket conformation for the SCCSCCS segment, with sulfurs pointing exo to the ring.[4] The ^1H NMR spectra of the ligand were also interpreted in favor of the bracket structure because of the magnitude of the *vic* coupling constants of the SCCS segments.[3] However molecular mechanics and molecular dynamics simulations of the ligand (gas phase) appeared to show that an all-gauche form with endo sulfur was close in energy.[3] Since, at that time, superior selectivity[1] in

(18) Shchori, E.; Jagur-Grodzinski, J; Shporer, M. *J. Am. Chem. Soc.* **1971**, *93*, 7133.
(19) Delville, A; Stöver, H. D. H.; Detellier, C. *J. Am. Chem. Soc.* **1987**, *109*, 7293.

ISE for silver had been observed with a series of analogous thiamacrocycles including L^1 and L^2, it was postulated[3] that an endo structure would permit coordination of the large silver ion, which might account for this selectivity. However, the subsequent observation of equally good selectivity for open-chain thioethers[7] requires a reconsideration of the earlier hypothesis.

The crystal structure of the silver chelate of L^1 reported in this paper clearly indicates that silver coordinates exo to the macrocycle, and the potential for silver to coordinate to each separate sulfur in this way is seen, in this instance leading to a polymeric complex of AgL stoichiometry. However, in solution, there is strong NMR evidence that H1, the unique proton which projects into the macrocycle cavity, is very strongly shifted on coordination to one silver ion for L^1 and L^2 (see Table 6) but not for L^3. The NMR spectra of the ligands in the presence of silver indicate a time-averaged symmetrical structure, and the proton coupling constants for the bracket section can no longer be determined by simulation since they appear as deceptively simple triplets. However the sum of the *vic* coupling constants ($J + J'$) can still be determined. The sum for the free L^1 was 17.66 Hz in $CDCl_3$ solution.[3] The corresponding sums $J + J'$ at the Ag/L ratios 1,2, and 3 were 12.25, 13.1, and 13.9 Hz for L^1 in CD_3CN. For free L^2, the ^1H spectrum again has deceptively simple triplets for the SCCO segment and the derived $J + J' = 14.4$ Hz, while the sum for the Ag/L ratio 1 is 11.54 Hz, increasing to 12.94 Hz for the ratio 3. Thus the conformations of both ligands clearly change with coordination to silver, with solvent, and with Ag/L ratio. The changes are consistent with a prevalence of *gauche* conformers in the SCCS(O)CCS bracket for the Ag/L complex of ratio 1, since the sum of coupling constants is lowest at that composition. It is intriguing that the sum of the coupling constants shows a consistent rise as the Ag/L ratio is raised to 3 in each instance. This is consistent with an increase in proportion of *anti* conformations in the bracket structure as sulfurs turn exo to the macrocycle to accommodate further silver ions which the crystal structure of Figure 1 shows to be possible. In solution at the AgL composition, we may simply be observing a bidentate S_2 coordination with the remaining coordination sites filled by solvent. This conformation has precedence in the X-ray structure of $[PdCl_2(L^1)]$.[5] The results may be interpreted as showing (i) an initial interaction which simply produces a Ag(η^1-L) complex with an all exodentate conformation, (ii) a rearrangement at the AgL composition to Ag(η^2-L) (shown in **I**), and then (iii) a rearrangement back to an all-exo conformation in the presence of excess Ag ion, analogous to the crystal structure.

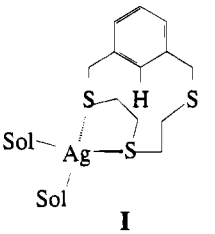

I

Selectivity and Kinetics. The mechanism is largely D or I_D based on the kinetic studies, which is in accord with the proposals of Armstrong and co-workers.[20] Selectivity thus probably arises from the slower dissociation of silver ions relative to those of other metals. The transport mechanism in the organic membrane of an ISE may thus by analogy be of the single carrier type and is unlikely to involve the so-called "Tarzan" mechanism in which the metal (Tarzan) switches from carrier to carrier (or rope to rope).

Conclusions

In relation to selectivity, ISE for silver ions based on L^1 or L^2 operate under liquid conditions in the presence of excess silver ions (from the contacting test solution and in the ISE membrane itself, in excess of ligand). On the basis of our structural data, it is suggested that structurally the preferred coordination to silver ions is exo in the crystal, while endo in solution, but the presence of excess silver ions may become exo. This may partly explain the particular selectivity of these macrocycles and is consistent also with the selectivity of open-chain ligands such as L^3 and L^4. Since L^3 selectivity for silver in ISE is equivalent to that of L^1 and L^2, yet does not show any special NMR shift for its H1 signal on coordination to silver, it is evident that any possible endo coordination of L^1 and L^2 to silver is not relevant to the selectivity process.

Acknowledgment. We acknowledge the Natural Sciences and Engineering Research Council of Canada, the Petroleum Research Fund, administered by the American Chemical Society, the Brite-Euram Programme of the EU, EPSRC, and CICYT Grant Mat 94-0668 from the Spanish Government for financial support of this research.

Supporting Information Available: Listings of crystallographic data collection parameters, positional parameters, thermal parameters, nonessential bonding parameters, and hydrogen atom parameters (5 pages). Ordering information is given on any current masthead page.

IC9503592

(20) Armstrong, R. D. A.; Todd, M. *Electrochim. Acta* **1987**, *32*, 1403.